ACS chemical biology

Articles

pubs.acs.org/acschemicalbiology

5′-*C*-Malonyl RNA: Small Interfering RNAs Modified with 5′-Monophosphate Bioisostere Demonstrate Gene Silencing Activity

Ivan Zlatev,[†] Donald J. Foster,[†] Jingxuan Liu,[†] Klaus Charisse,[†] Benjamin Brigham,[†] Rubina G. Parmar,[†] Vasant Jadhav,[†] Martin A. Maier,[†] Kallanthottathil G. Rajeev,[†] Martin Egli,[‡] and Muthiah Manoharan*[,†]

[†]Alnylam Pharmaceuticals, 300 Third Street, Cambridge, Massachusetts 02142, United States

[‡]Department of Biochemistry, Vanderbilt University, Nashville, Tennessee 37232, United States

Supporting Information

ABSTRACT: 5′-Phosphorylation is a critical step in the cascade of events that leads to loading of small interfering RNAs (siRNAs) into the RNA-induced silencing complex (RISC) to elicit gene silencing. 5′-Phosphorylation of exogenous siRNAs is generally accomplished by a cytosolic Clp1 kinase, and in most cases, the presence of a 5′-monophosphate on synthetic siRNAs is not a prerequisite for activity. Chemically introduced, metabolically stable 5′-phosphate mimics can lead to higher metabolic stability, increased RISC loading, and higher gene silencing activities of chemically modified siRNAs. In this study, we report the synthesis of 5′-*C*-malonyl RNA, a 5′-monophosphate bioisostere. A 5′-*C*-malonyl-modified nucleotide was incorporated at the 5′-terminus of chemically modified RNA oligonucleotides using solid-phase synthesis. *In vitro* silencing activity, *in vitro* metabolic stability, and *in vitro* RISC loading of 5′-*C*-malonyl siRNA was compared to corresponding 5′-phosphorylated and 5′-nonphosphorylated siRNAs. The 5′-*C*-malonyl siRNAs showed sustained or improved *in vitro* gene silencing and high levels of Ago2 loading and conferred dramatically improved metabolic stability to the antisense strand of the siRNA duplexes. *In silico* modeling studies indicate a favorable fit of the 5′-*C*-malonyl group within the 5′-phosphate binding pocket of human Ago2MID domain.

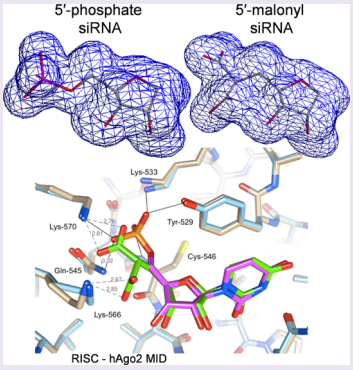

Introduced by Harris Friedman in 1950,[1] the concept of "bioisosteres" defines structurally different compounds that induce similar biological effects and has been widely exploited in drug design.[2,3] Bioisosteres involve the introduction of changes directed toward modulating or optimizing properties of drugs such as potency, selectivity, toxicity, and/or metabolic profile.[2] The concept of bioisosterism also provides a starting point for exploration of novel structural elements that offer an extensive palette in biomimicry-induced functionalities.[2,3]

As nucleotide and nucleic acid analogs have found an increasingly important place in modern drug discovery,[4−8] various bioisosteres of phosphate have been developed in order to mitigate the undesirable pharmacological features of the phosphate group.[2,9,10] The isosteres that have been explored include 5′-phosphonates,[9,11−13] squaric acid mono- and diamides designed as electronic mimetics,[14,15] and different acetal linkages probed as shape mimetics.[16−18] Recently, Herdewijn *et al.* developed a series of unique pyrophosphate mimics with electronic and topological isosterism with natural dNTPs.[19,20] Among these structures, several are efficiently incorporated into DNA by HIV-RT-1.[21] Smietana *et al.* reported the synthesis of a full series of 5′-borono-DNA nucleotides against human TMP kinase, carefully designed using semiempirical calculations as "nearly perfect mimic" of the natural 5′-monophosphates.[22]

We focus here on the use of 5′-monophosphate bioisosteres in RNA molecules that operate through the RNA interference (RNAi) pathway. RNAi is driven by Dicer-processed endogenous small interfering RNAs (siRNAs), which are 21−23 nucleotide-long RNA duplexes with 5′-monophosphates.[23,24] siRNAs are loaded into the polyprotein RNA-induced silencing complex (RISC), where the two RNA strands are dissociated, and the active antisense (guide) strand is loaded into the Argonaute-2 (Ago2) endonuclease. Upon Watson−Crick base pairing with target mRNA, Ago2 can cleave the mRNA target.[25−27] Synthetic siRNAs added exogenously operate through the same mechanism. A 5′-phosphate group on the antisense strand of the siRNA duplex is a requisite for optimal loading on to the RISC machinery;[28,29] after loading, the terminal phosphate is buried within the basic 5′-phosphate-binding pocket of the Ago2 MID domain. The 5′-terminal phosphate contributes to the antisense strand selectivity and its correct positioning for accurate mRNA cleavage.[30,31] Synthetic siRNAs bearing a 5′-hydroxyl (OH) group mediate RNAi function, as the siRNA is phosphorylated by an endogenous Clp1 kinase.[29] When phosphorylation at the 5′ end of the antisense strand is blocked, gene silencing is hampered.[9,31,32] A recent study from Kenski *et al.* have described the *in vivo* evaluation of liposome-formulated siRNAs bearing a synthetic 5′-phosphate compared to the nonphosphorylated versions.[33]

Received: August 12, 2015
Accepted: December 17, 2015
Published: December 17, 2015

DOI: 10.1021/acschembio.5b00654
ACS Chem. Biol. 2016, 11, 953−960

These siRNAs have similar *in vivo* activity, indicating that phosphorylation of the siRNA is not a rate-limiting step *in vivo*.[33] The addition of synthetic 5′-phosphate is necessary, however, in certain cases of extensively chemically modified siRNA duplexes that are not recognized by endogenous kinase.[29] It has been also shown that the presence of the 5′-phosphate group is of critical importance for reduction in mRNA levels triggered by single-stranded siRNAs.[27,32,34−36] Lima *et al.* analyzed the effects of several 5′-terminal modifications on the ss-siRNA activity *in vitro*.[9] The loss of natural 5′-phosphate *in vivo* due to phosphatase activity, the introduction of metabolically stable, phosphonate bioisosteres was required for efficient *in vivo* silencing.[9] Synthesis of such modified phosphate mimics is not trivial and requires multistep syntheses.

Use of unformulated, chemically modified siRNAs conjugated to *N*-acetylgalactosamine (GalNAc), which mediates uptake into hepatocytes, elicited RNAi mediated degradation of targeted mRNA in the hepatocytes following subcutaneous administration.[38] This approach for delivery of siRNAs has been recognized as therapeutically relevant, and the screening of novel chemical modifications on siRNA-GalNAc conjugates that increase RISC loading, gene silencing, and metabolic stability has become an important aspect in current and future siRNA drug design. Here, we describe the design and synthesis of a novel metabolically stable 5′-monophosphate bioisostere in siRNAs, the 5′-*C*-malonyl group. Malonyl phosphate mimetics have been successfully used in the small-molecule field, mainly as nonhydrolyzable phosphotyrosyl (pTyr) analogs.[39−41] To the best of our knowledge, use of these mimics has not yet been reported in the fields of nucleotide or oligonucleotide therapeutics.

RESULTS AND DISCUSSION

Choice of the 5′-Monophosphate Bioisostere and siRNA Design. We have identified a number of nonhydrolyzable phosphate mimics.[42] The 5′-*C*-malonyl group (Figure 1) is a promising 5′-phosphate bioisostere for several reasons. Due to the nonhydrolyzable *C*-*C* linkage to the terminal 5′-nucleotide of RNA, the 5′-*C*-malonyl should confer resistance to nuclease degradation, in particular to 5′-phosphatases and 5′-exonucleases. Like the 5′-phosphate, the 5′-*C*-malonyl is a dianion at physiological pH due to two acid dissociation constants, with pK_a values of the malonic acid being 2.83 and 5.69.[43] The malonate group is also known for its excellent chelating properties, and its mimicry of a pyrophosphate group.[20] Furthermore, free energy perturbation (FEP) calculations predict that 5′-*C*-malonyl adenosine requires more energy to desolvate but has more favorable interactions with the residues in the phosphate binding site of fructose 1,6-bisphosphatase when compared with adenosine 5′-monophosphate.[44] For the evaluation of 5′-*C*-malonyl RNA in the context of siRNAs, we chose to introduce the malonate-modified nucleotide at the 5′-extremity of the fully modified antisense strand of siRNAs targeted to silence expression of the human *phosphatase and tensin homologue* (*PTEN*) and the *apolipoprotein B* (*ApoB*) genes. The siRNA chemistry architecture is based on analysis of chemically modified siRNA in the context of GalNAc-siRNAs previously reported by our group.[38]

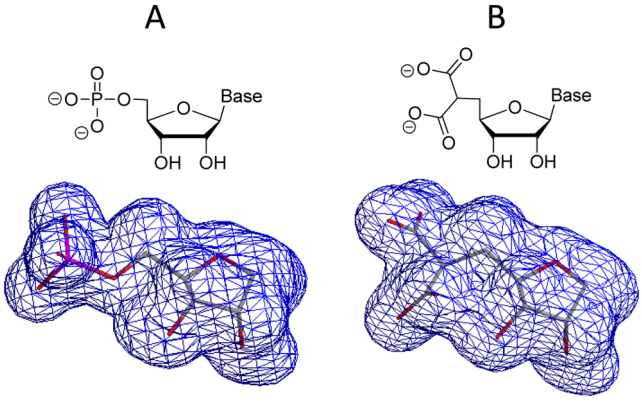

Figure 1. Chemical structures and calculated total surface charge density for (A) a 5′-monophosphate nucleoside and (B) a 5′-deoxy-5′-*C*-malonyl nucleoside. Generated using MM2 calculation for energy minimization and total surface charge density calculation functions on ChemBio 3D. Nucleobase and chemical modifications are not represented for simplicity.

Chemical Synthesis of 5′-*C*-Malonyl RNA. For the introduction of the 5′-*C*-malonyl group, we followed a procedure similar to the one previously described by Fiandor *et al.*,[45] namely an S_N2 reaction between a 5′-deoxy-5′-halonucleoside precursor and dialkyl malonate. The synthetic route is depicted in Scheme 1. The N^3-benzyloxymethyl (BOM) protected uridine derivative **2** was obtained in quantitative yield from the commercially available 2′-*O*-methyl-3′-*O*-*tert*-butyldimethylsilyl-uridine (**1**) upon treatment with BOM-chloride.[46,47] The BOM protection on N^3 in **2** was preferred over the previously used benzyl[45] as it can be more readily removed under hydrogenolysis conditions. The N^3-BOM protected nucleoside **2** was converted to the corresponding 5′-deoxy-5′-iodo nucleoside **3** in one step in 92% yield. The 5′-iodide **3** was then efficiently substituted with the malonyl anion generated *in situ* from dimethyl malonate and sodium methoxide (Scheme 1), resulting in a fully protected 5′-deoxy-5′-*C*-malonyl nucleoside **4** in 92% yield. Subsequent deprotection of the N^3-BOM group on **4** using 10% Pd/C under a hydrogen atmosphere in the presence of catalytic formic acid in isopropanol/water,[48] followed by removal of the 3′-*O*-TBS group, afforded the nucleoside precursor **6**. Finally, phosphitylation of the 3′-hydroxyl group of **6** under standard conditions afforded the phosphoramidite **7** as the monomer building block for oligonucleotide synthesis. In addition, we also prepared the fully deprotected 5′-deoxy-5′-*C*-malonyl nucleoside **8** using the conditions applied for 5′-*C*-malonyl oligonucleotide deprotection: treatment by 1 M aqueous piperidine, followed by aqueous ammonia/ethanol treatment at RT. Using these conditions, complete deprotection of the malonate methyl esters was achieved, and no decarboxylation of the free diacid was observed. HRMS analysis confirmed complete hydrolysis of the methyl esters on **6** to the corresponding diacid **8** under this condition without any aminolysis.

Oligonucleotide synthesis was performed on an oligonucleotide synthesizer. The 5′-deoxy-5′-*C*-(dimethylmalonyl)-2′-*O*-methyluridine-3′-*O*-phosphoramidite (**7**) was coupled as the 5′-terminal nucleotide to yield protected, full-length oligonucleotides. For the 5′-*C*-malonyl oligonucleotides, the two-step deprotection procedure involved initial treatment with 1 M aqueous piperidine for 24 h, followed by evaporation of piperidine and a subsequent treatment with aqueous ammonia/ethanol for 36 h. It was critical to perform these deprotections

DOI: 10.1021/acschembio.5b00654
ACS Chem. Biol. 2016, 11, 953−960

Scheme 1. Synthesis of 5′-Deoxy-5′-*C*-malonyl Nucleoside Monomer[a]

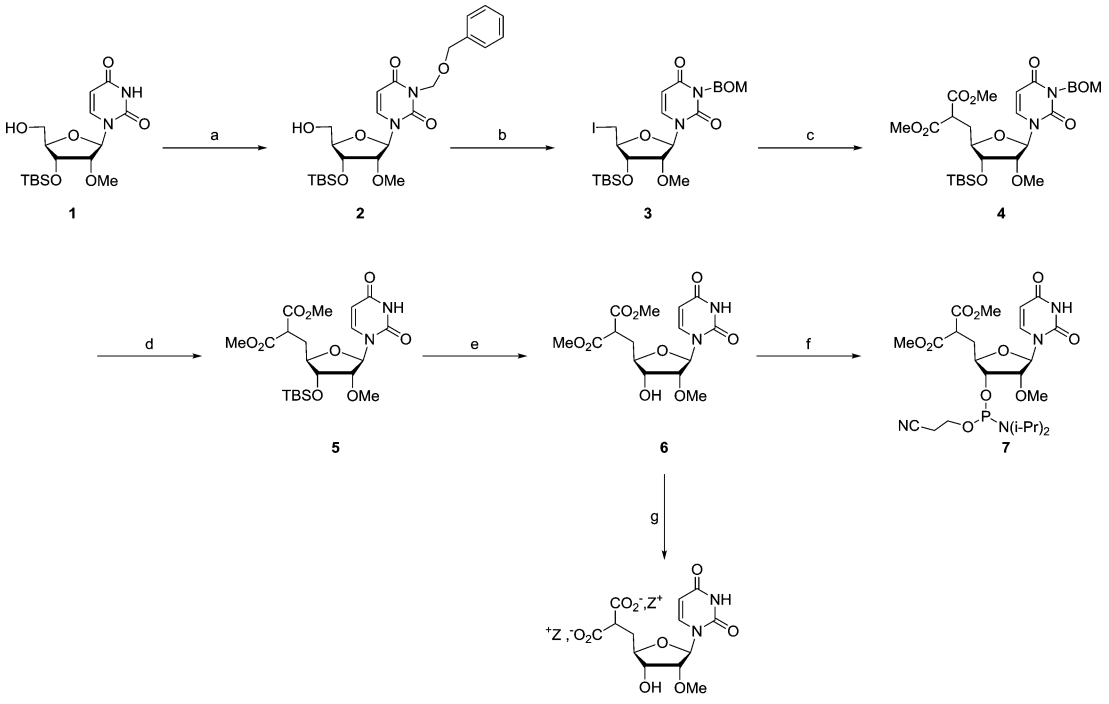

[a]Reagents and conditions: (a) BOM-chloride, DBU, DMF, 30 min, 0 °C, quant.;[46,47] (b) methyltriphenoxyphosphonium iodide, DMF, 15 min, rt, 92%;[49] (c) sodium methoxide, dimethyl malonate, 1,2-DME, 24 h, reflux, 92%; (d) 10% Pd/C, H_2 atm, i-PrOH/H_2O (10:1, v/v), 0.05 equiv formic acid, 12 h, rt, 98%;[48] (e) NEt_3-3HF, THF, 48 h, rt, 88%; (f) 2-cyanoethyl *N*,*N*-diisopropylchlorophosphoramidite, DIEA, DCM, 18 h, rt, 56%; (g) 1 M aq. piperidine, 24 h, rt; then 30% aq. ammonia/ethanol (3:1, v/v), 36 h, rt, quant., Z^+ = piperidinium.

Table 1. IC_{50} Values for 5′-*C*-Malonyl, 5′-Phosphate, and 5′-OH siRNAs in *PTEN* and *ApoB* Silencing in Cell-based Assays

siRNA target	5′-modification	sense strand (5′-3′)[a]	antisense strand (5′-3′)[a]	IC_{50} (nM)[b]
1 ApoB	OH	*C*•c•*UgGaCaUUCaGaAcAaGaA*-GalNAc	u•*U*•c*UuGuUcUgaaUgUcCaGg*•g•u	1.03 ± 0.52
2 ApoB	phosphate	*C*•c•*UgGaCaUUCaGaAcAaGaA*-GalNAc	**Pu**•*U*•c*UuGuUcUgaaUgUcCaGg*•g•u	0.13 ± 0.03
3 ApoB	OH	*U*•g•*UgAcAaAUAuGgGcAuCaA*-GalNAc	u•*U*•g*AuGcCcAuauUuGuCaCa*•a•a	0.50 ± 0.21
4 ApoB	phosphate	*U*•g•*UgAcAaAUAuGgGcAuCaA*-GalNAc	**Pu**•*U*•g*AuGcCcAuauUuGuCaCa*•a•a	0.13 ± 0.03
5 ApoB	malonate	*C*•c•*UgGaCaUUCaGaAcAaGaA*-GalNAc	**Mu**•*U*•c*UuGuUcUgaaUgUcCaGg*•g•u	0.71 ± 0.41
6 ApoB	malonate	*U*•g•*UgAcAaAUAuGgGcAuCaA*-GalNAc	**Mu**•*U*•g*AuGcCcAuauUuGuCaCa*•a•a	0.40 ± 0.22
7 PTEN	OH	*AaGuAaGgAcCaGaGaCaAdT*•dT	u*UgUcUcUgGuCcUuAcUud*T•dT	0.71 ± 0.19
8 PTEN	phosphate	*AaGuAaGgAcCaGaGaCaAdT*•dT	**Pu***UgUcUcUgGuCcUuAcUud*T•dT	0.24 ± 0.01
9 PTEN	malonate	*AaGuAaGgAcCaGaGaCaAdT*•dT	**Mu***UgUcUcUgGuCcUuAcUud*T•dT	0.22 ± 0.02

[a]**P** indicates 5′-monophosphate; **M** indicates 5′-malonate; italicized upper case and normal lower case letters indicate 2′-deoxy-2′-fluoro (2′-F) and 2′-*O*-methyl (2′-OMe) sugar modifications, respectively; • indicates phosphorothioate (PS) linkage; dT indicates 2′-deoxythymidine nucleotide; GalNAc indicates hydroxyprolynyl trivalent *N*-acetyl-galactosamine ligand.[38] [b]Half maximal inhibitory concentration (IC_{50}) for gene silencing in primary mouse hepatocytes. All values are from triplicate experiments. Mean values ± SEM are reported.

at RT (~25 °C) in order to avoid decarboxylation of the malonic acid.

***In Vitro* Gene Silencing.** The 5′-*C*-malonyl siRNAs were evaluated *in vitro* against two different targets, *ApoB* and *PTEN* (Table 1). To investigate the effect of chemical phosphorylation/phosphate mimicry at the 5′-end of siRNAs antisense strands, siRNA duplexes with 5′-*C*-malonyl, 5′-phosphate, and 5′-OH termini were synthesized. The siRNAs were fully chemically modified with alternating 2′-deoxy-2′-fluoro (2′-F) and 2′-*O*-methyl (2′-OMe) sugar-modified nucleotides. In the case of siRNA sequences targeting *ApoB* (siRNAs **1**−**6 ApoB**), we prepared GalNAc-siRNA conjugates as previously described.[38] The *ApoB*-targeting GalNAc-siRNAs were delivered into primary mouse hepatocytes by transfection, and gene silencing was measured as a function of siRNA concentration (Table 1). We observed a strong discrimination between 5′-phosphorylated and 5′-nonphosphorylated siRNA duplexes. For each of the two *ApoB* sequences evaluated, the 5′-phosphate siRNAs had 5- to 10-fold higher potency than the nonphosphorylated siRNA. The 5′-*C*-malonyl phosphate mimic siRNAs showed levels of *ApoB* gene silencing somewhat inferior to that observed with the 5′-phosphate siRNAs (Table 1) but similar to that of the nonphosphorylated siRNAs. The 5′-malonyl and 5′-phosphate *PTEN* targeting siRNAs conferred similar advantages relative to the nonphosphorylated siRNA. Both were approximately 3-fold more potent than the 5′-OH *PTEN* siRNA (Table 1 and Figure 2). The difference in potency between 5′-nonphosphorylated and 5′-phosphorylated (or phosphate mimic) siRNAs is possibly sequence dependent and is likely due to differences in 5′-phosphorylation

DOI: 10.1021/acschembio.5b00654
ACS Chem. Biol. 2016, 11, 953−960

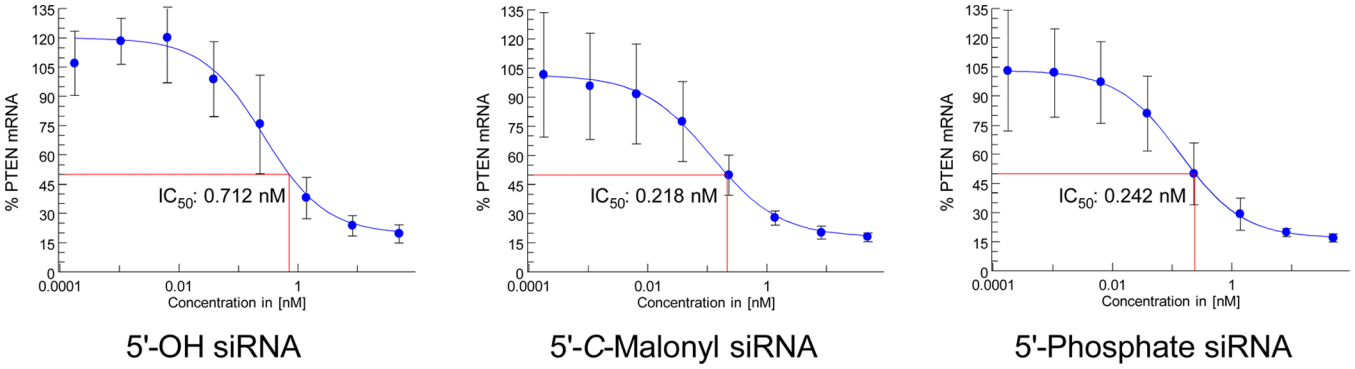

Figure 2. Dose–response curves for 5′-OH, 5′-*C*-malonyl, and 5′-phosphate *PTEN* siRNAs in primary mouse hepatocytes. All values are from triplicate experiments.

efficiencies in the cells.[29] In the case of the PTEN siRNA, the 5′-*C*-malonyl phosphate mimic siRNAs performed better than its 5′-nonphosphorylated counterpart.

It is evident from our results that *in vitro* potency of extensively modified siRNAs, currently being used in the context of GalNAc-siRNA conjugates,[38] depends on the presence or absence of the 5′-phosphate. The introduction of 5′-phosphate bioisosteres that preserve the intrinsic RNAi gene silencing potency and confer higher metabolic stability would be of particular interest for siRNAs used clinically. siRNAs chemically synthesized with a natural 5′-phosphate are not suitable for *in vivo* application, as the terminal 5′-phosphate is swiftly removed *in vivo* by the actions of phosphatases.[9]

Tritosome Stability of 5′-*C*-Malonyl siRNAs. To evaluate the stability of 5′-*C*-malonyl siRNAs, we used a rat liver tritosome assay. Liver tritosomes are used as a model for lysosomes.[50] siRNA duplexes were incubated with rat liver tritosomes for 4 and 24 h, and levels of individual strands of the siRNA duplex quantified as full-length single strands were evaluated using HPLC/MS (Supporting Information). The 5′-*C*-malonyl isostere conferred a dramatic increase in metabolic stability relative to the 5′-phosphate- and 5′-OH-containing antisense strands (Figure 3). The antisense strand of siRNA **9 PTEN** was intact after 24 h, whereas the full-length antisense strands of the 5′-OH (**7 PTEN**) or the 5′-phosphate (**8 PTEN**) siRNAs remained undetectable level after 4 h of incubation (Figure 3). The increased stability of the 5′-*C*-malonyl antisense strand did not stabilize the sense strand significantly,

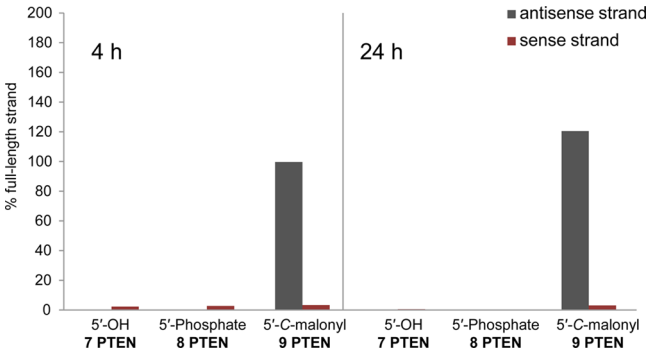

Figure 3. Stabilities of 5′-*C*-malonyl, 5′-phosphate, and 5′-OH siRNAs incubated in rat liver tritosomes. siRNAs were incubated at 0.4 mg mL^{-1} (*ca.* 5 μM) concentration for 4 and 24 h in the presence of tritosomes. Percent full-length strand was determined by HPLC. Data were normalized to untreated controls.

as very little of the full-length **9 PTEN** sense strand was detected after 4 h of incubation with tritosomes (Figure 3). However, significant stabilization of the 5′ N-1 sense strand was observed in the case of the stabilized **9 PTEN** 5′-*C*-malonyl siRNA duplex, even after 24 h of incubation (Figure S1, Supporting Information). This observation demonstrates that a metabolically stable antisense strand did not fully protect the sense strand by stabilizing the entire duplex siRNA. However, after cleavage of the 5′-terminal nucleotide of the sense strand, the 5′-*C*-malonyl antisense strand, by its inherently higher stability toward 5′-exonuclease degradation, was able to stabilize the N-1 sense strand containing duplex, possibly by maintaining the daughter duplex integrity and hence exerting more resistance to nucleolytic attacks.

RNA taken up by hepatocytes is degraded in lysosomes.[51,52] An acid endoribonuclease, a nonspecific acid nucleotidase (phosphatase), and an acid 5′-OH-specific phosphodiesterase (5′-exonuclease) are the primary actors of RNA degradation in lysosomes.[52] It is likely that a 5′-phosphorylated siRNA duplex will be rapidly dephosphorylated, resulting in the 5′-OH siRNA, which becomes a target for the lysosomal 5′-OH-specific phosphodiesterase. The 5′-deoxy-5′-*C*-malonyl group exerts protection against both the phosphatase and the 5′-exonuclease. The 5′-*C*-malonyl group thus appears to be an excellent 5′-phosphate bioisostere by significantly enhancing the metabolic stability of the antisense strand of siRNAs and by retaining gene silencing activity.

***In Vitro* Ago2 Loading of 5′-*C*-Malonyl siRNAs.** To understand the mechanistic features that enable recognition of the 5′-*C*-malonyl bioisostere by the RISC machinery, we analyzed the interaction of 5′-*C*-malonyl-modified siRNA with Ago2 by immunoprecipitation and molecular modeling. The 5′-*C*-malonyl antisense strand was efficiently loaded on RISC confirmed by Ago2 immunoprecipitation from primary mouse hepatocytes transfected with siRNAs. Primary hepatocytes were transfected with 5′-*C*-malonyl, 5′-phosphate, and 5′-OH *PTEN*-targeting siRNAs. Ago2 protein was immunoprecipitated from cell lysate after 24 h, and the amount of single strands coimmunoprecipitated were determined by RT-PCR. As shown in Figure 4, each of the siRNAs was loaded on RISC. The 5′-*C*-malonyl siRNA antisense strand was present at 3.8-fold higher levels than the 5′-OH and 5′-phosphate siRNAs. Interestingly, the *in vitro* gene silencing potencies of the 5′-*C*-malonyl and 5′-phosphate PTEN siRNAs were similar (Table 1 and Figure 2). A plausible explanation of not showing improved potency by the modified siRNA despite higher RISC loading is poor catalytic efficiency of the malonylated antisense strand loaded

DOI: 10.1021/acschembio.5b00654
ACS Chem. Biol. 2016, 11, 953–960

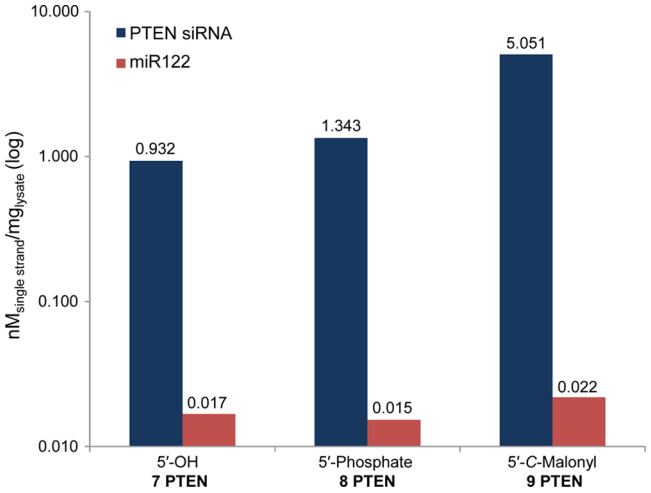

Figure 4. RISC loaded antisense strands 5′-*C*-malonyl, 5′-phosphate, and 5′-OH siRNAs determined by immunoprecipitation of Ago2 from primary mouse hepatocytes and by RT-PCR amplification of the Ago2-loaded single strands. siRNAs **7**, **8**, and **9** were transfected into cells at 10 nM. Levels of antisense strands are based on incubated nM siRNA per milligram of cell lysate. Levels of endogenous miR122 were determined as controls.

RISC compared to the 5′-phosphorylated siRNA. Although correlation between RISC loading and *in vitro* potency or *in vitro* stability cannot be clearly established using this analysis, the data demonstrate that the 5′-*C*-malonyl isostere-modified siRNA was recognized *in vitro* by Ago2.

***In Silico* Model of the Complex between 5′-Deoxy-5′-*C*-malonyluridine and the hAgo2MID Domain.** The interactions of a 5′-deoxy-5′-*C*-malonyluridine at the NMP binding site of the hAgo2MID domain[53] were modeled using a molecular mechanics approach (Amber force field in UCSF Chimera[54]). The 5′-phosphate of UMP in the crystal structure of the MID domain complex makes hydrogen-bond-mediated contacts with Tyr529, Lys533, Gln545, Cys546, and Lys570 (Figure 5). The malonyl carboxylates in the modeled complex are contacted by Gln545, Lys566, and Lys570. Thus, the malonyl moiety displays a slight shift relative to the standard phosphate and likely makes fewer contacts with the protein. The malonyl is farther from Tyr529 (4.05 Å between the tyrosine hydroxyl oxygen and one of the carboxylate oxygens) and Lys533 (4.85 Å between Nζ and the same malonyl oxygen) than the phosphate. Interestingly, in the complex between hAgo2 and miR-20a, Lys566 also contributes to the recognition of the 5′-phosphate moiety (see Figure 5B in cited ref 55); in our 5′-malonyl model, this interaction is observed. The 5′-malonyl group was successfully accommodated within the hAgo2MID binding pocket; no steric or electronic-clash interactions between enzyme and phosphate mimic were observed. Hydrogen bonds with two of the five residues that interact with the 5′ phosphate of UMP likely also form between 5′-malonyl and the protein. The more limited interaction mode of 5′-malonyl compared to 5′-phosphate is in line with the slight reduction of *in vitro* potency observed between some 5′-phosphate and 5′-malonate siRNAs (Table 1).

CONCLUSIONS

Various phosphate bioisostere groups have been synthesized, but few have been evaluated in therapeutic RNA molecules. 5′-Phosphorylation of siRNAs is a critical step for RNAi-mediated

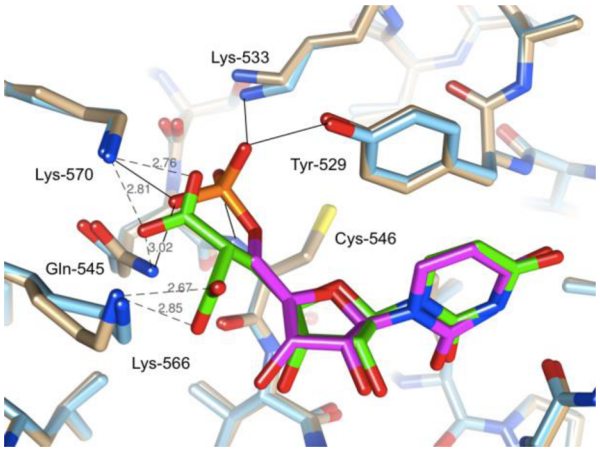

Figure 5. Superimposition of the modeled complex between 5′-deoxy-5′-*C*-malonyluridine (carbon atoms colored in green) and the hAgo2MID domain (gray carbon atoms) and the crystal structure of UMP (magenta carbons) complexed with the MID (light blue carbons) complex.[53] The Matchmaker option in UCSF Chimera[54] was used to generate the overlay. Key residues are labeled. H-bonds stabilizing the 5′-malonyl moiety are dashed black lines with distances in Å indicated, and H-bonds stabilizing the 5′-phosphate are thin solid lines. Hydrogen atoms were omitted from the modeled complex for clarity.

gene silencing. In this study, we described the synthesis of a novel metabolically stable 5′-monophosphate bioisostere, the 5′-*C*-malonyl group. The modification was incorporated at the 5′ terminus of the antisense strand of double stranded siRNAs. These 5′-*C*-malonyl siRNAs silenced expression of two different genes, *PTEN* and *ApoB*, in primary mouse hepatocytes as effectively as or more effectively than corresponding 5′-phosphate or 5′-OH siRNAs. The 5′-malonate phosphate mimic conferred significant increase in the metabolic stability of siRNA duplexes in lysosomal matrices. siRNAs with a malonyl moiety at the 5′-end of antisense strand were recognized by the MID domain, the phosphate-binding pocket of Ago2, as evident from efficient loading of the modified antisense strand into RISC *in vitro*, confirmed by Ago2 immunoprecipitation. The *in silico* molecular modeling studies showed a favorable fit of the 5′-*C*-malonyl group within the 5′-phosphate binding site of the MID domain of human Ago2. When taken together, these results indicate that the 5′-*C*-malonyl, a metabolically stable 5′-phosphate bioisostere, has excellent biomimicry properties and high potential for use in therapeutic siRNAs. We anticipate that use of the 5′-malonyl phosphate mimic will significantly enhance the therapeutic value of future RNAi-based drugs.

METHODS

Cell Culture and Transfection. Primary mouse hepatocytes were obtained from Life Technologies and cultured in Williams E Medium with 10% fetal bovine serum (FBS). Transfection was carried out by adding 4.9 μL of Opti-MEM plus 0.1 μL of Lipofectamine RNAiMax (Invitrogen) per well to 5 μL of each siRNA duplex at the desired concentration to an individual well in a 384-well plate. The mixture was incubated at RT for 20 min, and 40 μL of complete growth media containing 5000 cells was added to the siRNA mixture. Cells were incubated for 24 h prior to RNA isolation. A similar procedure was followed for the transfection of 10 000 000 cells and scaled accordingly. Dose response experiments were done using eight 6-fold serial dilutions over the range of 20 nM to 75 pM or 50 nM to 187.5 pM.

DOI: 10.1021/acschembio.5b00654
ACS Chem. Biol. 2016, 11, 953−960

RNA Isolation. RNA was isolated using a Dynabeads mRNA Isolation Kit (Invitrogen). Cells were lysed in 75 μL of Lysis/Binding Buffer containing 3 μL of beads per well and mixed for 10 min on an electrostatic shaker. Buffers were prepared according to the manufacturer's protocol. The washing steps were automated on a Biotek EL406 using a magnetic plate support. Beads were washed (90 μL) once in buffer A, once in buffer B, and twice in buffer E, with aspiration steps between washes.

cDNA Synthesis. cDNA synthesis was accomplished with the ABI High capacity cDNA reverse transcription kit (Applied Biosystems). A mixture of 1 μL of 10× buffer, 0.4 μL of 25× dNTPs, 1 μL of random primers, 0.5 μL of reverse transcriptase, 0.5 μL of RNase inhibitor, and 6.6 μL of water per reaction were added per well. Plates were sealed, agitated for 10 min on an electrostatic shaker, and then incubated at 37 °C for 2 h. Following this, the plates were agitated at 80 °C for 8 min.

Real-time PCR. cDNA (2 μL) was added to a master mix containing 0.5 μL mouse GAPDH TaqMan Probe (Applied Biosystems, Cat.# 4308313), 0.5 μL of mouse *ApoB* or *PTEN* TaqMan probes (Applied Biosystems, Cat.# Mm01545156_m1 and Mm01212532_m1, respectively), and 5 μL of Lightcycler 480 probe master mix (Roche) per well in a 384-well 50 plate (Roche). Real-time PCR was done in an ABI 7900HT RT-PCR system (Applied Biosystems) using the ΔΔCt (RQ) assay. Each duplex and concentration was tested in four biological replicates. To calculate relative fold change, real time data were analyzed using the ΔΔCt method and normalized to assays performed with cells transfected with 10 nM nonspecific siRNA. IC_{50} values were calculated using a four-parameter fit model using XLFit.

Tritosome Stability Assay. Rat liver tritosomes (Xenotech, custom product PR14044) were thawed to RT and diluted to 0.5 units mL^{-1} in 20 mM sodium citrate buffer, pH 5.0. Samples were prepared by mixing 100 μL of 0.5 units mL^{-1} acid phosphatase tritosomes with 25 μL of 0.4 mg mL^{-1} siRNA in a microcentrifuge tube. After incubation for 4 or 24 h in an Eppendorf Thermomixer set to 37 °C and 300 rpm, 300 μL of Phenomenex Lysis Loading Buffer and 12.5 μL of a 0.4 mg mL^{-1} internal standard siRNA were added to each sample. Samples for time 0 were prepared by mixing 100 μL of 0.5 units mL^{-1} acid phosphatase Tritosomes with 25 μL of 0.4 mg mL^{-1} siRNA sample, 300 μL of Phenomenex Lysis Loading Buffer, and 12.5 μL of a 0.4 mg mL^{-1} internal standard siRNA. siRNA was extracted from each time point sample (0 h, 4 h, 24 h) using a Phenomenex Clarity OTX Starter Kit. The samples were then resuspended with 500 μL of nuclease free water, and 50 μL of sample was analyzed by LC/MS. Analytical procedures and LC/MS plots are included as Supporting Information.

RISC Immunoprecipitation and RT-PCR Assay. siRNA-transfected primary mouse hepatocytes (10 000 000 cells) were lysed in lysis buffer (50 mM Tris-HCl, pH 7.5, 100 mM NaCl, 1% NP-40, 0.1% SDS) with protease inhibitor (Sigma-Aldrich). Lysate concentration was measured with a protein BCA kit (Thermo Scientific). For each reaction, 2 mg of total lysate was used. Anti-Ago2 antibody was purchased from Wako Chemicals (Clone No.: 2D4). Control mouse IgG was from Santa Cruz Biotechnology (sc-2025). Dynabeads (Life Technologies) were used to precipitate antibodies. Ago2-associated siRNA and endogenous miR122 were measured by Stem-Loop RT followed by TaqMan PCR analysis based on previously published methods.[56]

Computational Simulation of the Interaction between 5′-Deoxy-5′-*C*-malonyluridine and the Human Ago2MID Domain. The recognition modes of available crystal structures of complexes between hAgo2MID (amino acids 432−578; residues 440−572 are resolved in the electron density) and UMP (PDB ID code 3LUJ)[53] and full-length hAgo2 and miR-20a (PDB ID code 4F3T)[55] revealed that the recognition modes of 5′-terminal phosphates are very similar. The only difference between the two structures is that in the complex with full-length Ago2, a residue from the PIWI domain (Arg812) makes a contribution to the recognition of the 5′-phosphate. We therefore used the UMP:MID complex as the basis for modeling the interaction between 5′-malonyluridine and the hAgo2MID domain. Three-dimensional coordinates of the UMP:MID complex were retrieved from the Protein Data Bank (http://www.rcsb.org). Using the program UCSF Chimera (version 1.5.3),[54] all water molecules from the crystal structure were deleted, and the 5′-phosphate group was converted to the 5′-*C*-malonyl moiety. Hydrogen atoms were then added and the geometry of 5′-deoxy-5′-*C*-malonyluridine and its orientation and H-bonding/nonbonded interactions at the 5′-phosphate pocket of the hAgo2MID domain optimized with the Amber force field (ff12SB and Gasteiger charges for standard amino acids and nonstandard residues, respectively), as implemented in UCSF Chimera.

■ ASSOCIATED CONTENT

Supporting Information

The Supporting Information is available free of charge on the ACS Publications website at DOI: 10.1021/acschembio.5b00654.

Detailed experimental procedures and analytical data for compounds and oligonucleotides, NMR spectra of compounds, and LC/MS data for tritosome assay (PDF)

Accession Codes

PDB: 3LUJ, 4F3T.

■ AUTHOR INFORMATION

Corresponding Author

*Tel.: +1 617 551 8319. Fax: +1 617 551 8102. E-mail: mmanoharan@alnylam.com.

Funding

Alnylam Pharmaceuticals.

Notes

The authors declare the following competing financial interest(s): All Alnylam authors except B.B. are current employees of the company.

■ ACKNOWLEDGMENTS

The authors thank F. Morvan (Université de Montpellier) for helpful discussions.

■ REFERENCES

(1) Friedman, H. L. (1951) *Influence of Isosteric Replacements upon Biological Activity*, vol *206*, pp 295−358, National Academy of Sciences-National Research Council Publication, Washington, DC.

(2) Meanwell, N. A. (2011) Synopsis of Some Recent Tactical Application of Bioisosteres in Drug Design. *J. Med. Chem. 54*, 2529−2591.

(3) Patani, G. A., and LaVoie, E. J. (1996) Bioisosterism: A Rational Approach in Drug Design. *Chem. Rev. 96*, 3147−3176.

(4) De Clercq, E. (2009) The history of antiretrovirals: key discoveries over the past 25 years. *Rev. Med. Virol. 19*, 287−299.

(5) Uhlmann, E., and Peyman, A. (1990) Antisense oligonucleotides: a new therapeutic principle. *Chem. Rev. 90*, 543−584.

(6) de Fougerolles, A., Vornlocher, H.-P., Maraganore, J., and Lieberman, J. (2007) Interfering with disease: a progress report on siRNA-based therapeutics. *Nat. Rev. Drug Discovery 6*, 443−453.

(7) Burnett, J. C., Rossi, J. J., and Tiemann, K. (2011) Current progress of siRNA/shRNA therapeutics in clinical trials. *Biotechnol. J. 6*, 1130−1146.

(8) Bumcrot, D., Manoharan, M., Koteliansky, V., and Sah, D. W. Y. (2006) RNAi therapeutics: a potential new class of pharmaceutical drugs. *Nat. Chem. Biol. 2*, 711−719.

(9) Lima, W. F., Prakash, T. P., Murray, H. M., Kinberger, G. A., Li, W., Chappell, A. E., Li, C. S., Murray, S. F., Gaus, H., Seth, P. P., Swayze, E. E., and Crooke, S. T. (2012) Single-Stranded siRNAs Activate RNAi in Animals. *Cell 150*, 883−894.

DOI: 10.1021/acschembio.5b00654
ACS Chem. Biol. 2016, 11, 953−960

(10) Elliott, T. S., Slowey, A., Ye, Y., and Conway, S. J. (2012) The use of phosphate bioisosteres in medicinal chemistry and chemical biology. *MedChemComm 3*, 735−751.
(11) Gallier, F., Alexandre, J. A. C., El Amri, C., Deville-Bonne, D., Peyrottes, S., and Périgaud, C. (2011) 5′,6′-Nucleoside Phosphonate Analogues Architecture: Synthesis and Comparative Evaluation towards Metabolic Enzymes. *ChemMedChem 6*, 1094−1106.
(12) Gallier, F., Lallemand, P., Meurillon, M., Jordheim, L. P., Dumontet, C., Périgaud, C., Lionne, C., Peyrottes, S., and Chaloin, L. (2011) Structural Insights into the Inhibition of Cytosolic 5′-Nucleotidase II (cN-II) by Ribonucleoside 5′-Monophosphate Analogues. *PLoS Comput. Biol. 7*, e1002295.
(13) Pradere, U., Amblard, F., Coats, S. J., and Schinazi, R. F. (2012) Synthesis of 5′-Methylene-Phosphonate Furanonucleoside Prodrugs: Application to D-2′-Deoxy-2′-α-fluoro-2′-β-C-methyl Nucleosides. *Org. Lett. 14*, 4426−4429.
(14) Sato, K., Seio, K., and Sekine, M. (2002) Squaryl Group as a New Mimic of Phosphate Group in Modified Oligodeoxynucleotides: Synthesis and Properties of New Oligodeoxynucleotide Analogues Containing an Internucleotidic Squaryldiamide Linkage. *J. Am. Chem. Soc. 124*, 12715−12724.
(15) Seio, K., Miyashita, T., Sato, K., and Sekine, M. (2005) Synthesis and Properties of New Nucleotide Analogues Possessing Squaramide Moieties as New Phosphate Isosters. *Eur. J. Org. Chem. 2005*, 5163−5170.
(16) Pudlo, J. S., Cao, X., Swaminathan, S., and Matteucci, M. D. (1994) Deoxyoligonucleotides containing 2′,5′ acetal linkages: Synthesis and hybridization properties. *Tetrahedron Lett. 35*, 9315−9318.
(17) Lin, K.-Y., and Matteucci, M. D. (1996) The synthesis and hybridization properties of an oligonucleotide containing hexafluoroacetone ketal internucleotide linkages. *Tetrahedron Lett. 37*, 8667−8670.
(18) Zou, R., and Matteucci, M. D. (1996) Synthesis and hybridization properties of an oligonucleotide analog containing a glucose-derived conformation-restricted ribose moiety and 2′, 5′ formacetal linkages. *Tetrahedron Lett. 37*, 941−944.
(19) Adelfinskaya, O., and Herdewijn, P. (2007) Amino Acid Phosphoramidate Nucleotides as Alternative Substrates for HIV-1 Reverse Transcriptase. *Angew. Chem., Int. Ed. 46*, 4356−4358.
(20) Zlatev, I., Giraut, A., Morvan, F., Herdewijn, P., and Vasseur, J.-J. (2009) δ-Di-carboxybutyl phosphoramidate of 2′-deoxycytidine-5′-monophosphate as substrate for DNA polymerization by HIV-1 reverse transcriptase. *Bioorg. Med. Chem. 17*, 7008−7014.
(21) Herdewijn, P., and Marlière, P. (2012) Redesigning the leaving group in nucleic acid polymerization. *FEBS Lett. 586*, 2049−2056.
(22) El Amri, C., Martin, A. R., Vasseur, J.-J., and Smietana, M. (2012) Borononucleotides as Substrates/Binders for Human NMP Kinases: Enzymatic and Spectroscopic Evaluation. *ChemBioChem 13*, 1605−1612.
(23) Zamore, P. D., Tuschl, T., Sharp, P. A., and Bartel, D. P. (2000) RNAi: Double-Stranded RNA Directs the ATP-Dependent Cleavage of mRNA at 21 to 23 Nucleotide Intervals. *Cell 101*, 25−33.
(24) Elbashir, S. M., Harborth, J., Lendeckel, W., Yalcin, A., Weber, K., and Tuschl, T. (2001) Duplexes of 21-nucleotide RNAs mediate RNA interference in cultured mammalian cells. *Nature 411*, 494−498.
(25) Ketting, R. F. (2011) The Many Faces of RNAi. *Dev. Cell 20*, 148−161.
(26) Filipowicz, W. (2005) RNAi: The Nuts and Bolts of the RISC Machine. *Cell 122*, 17−20.
(27) Lima, W. F., Murray, H., Nichols, J. G., Wu, H., Sun, H., Prakash, T. P., Berdeja, A. R., Gaus, H. J., and Crooke, S. T. (2009) Human Dicer Binds Short Single-strand and Double-strand RNA with High Affinity and Interacts with Different Regions of the Nucleic Acids. *J. Biol. Chem. 284*, 2535−2548.
(28) Nykänen, A., Haley, B., and Zamore, P. D. (2001) ATP Requirements and Small Interfering RNA Structure in the RNA Interference Pathway. *Cell 107*, 309−321.
(29) Manoharan, M. (2004) RNA interference and chemically modified small interfering RNAs. *Curr. Opin. Chem. Biol. 8*, 570−579.
(30) Jinek, M., and Doudna, J. A. (2009) A three-dimensional view of the molecular machinery of RNA interference. *Nature 457*, 405−412.
(31) Chen, P. Y., Weinmann, L., Gaidatzis, D., Pei, Y., Zavolan, M., Tuschl, T., and Meister, G. (2008) Strand-specific 5′-O-methylation of siRNA duplexes controls guide strand selection and targeting specificity. *RNA 14*, 263−274.
(32) Martinez, J., Patkaniowska, A., Urlaub, H., Lührmann, R., and Tuschl, T. (2002) Single-Stranded Antisense siRNAs Guide Target RNA Cleavage in RNAi. *Cell 110*, 563−574.
(33) Kenski, D. M., Willingham, A. T., Haringsma, H. J., Li, J. J., and Flanagan, W. M. (2012) In Vivo Activity and Duration of Short Interfering RNAs Containing a Synthetic 5′-Phosphate. *Nucleic Acid Ther. 22*, 90−95.
(34) Haringsma, H. J., Li, J. J., Soriano, F., Kenski, D. M., Flanagan, W. M., and Willingham, A. T. (2012) mRNA knockdown by single strand RNA is improved by chemical modifications. *Nucleic Acids Res. 40*, 4125−36.
(35) Kini, H. K., and Walton, S. P. (2007) In vitro binding of single-stranded RNA by human Dicer. *FEBS Lett. 581*, 5611−5616.
(36) Schwarz, D. S., Hutvagner, G., Haley, B., and Zamore, P. D. (2002) Evidence that siRNAs function as guides, not primers, in the Drosophila and human RNAi pathways. *Mol. Cell 10*, 537−548.
(37) Prakash, T. P., Lima, W. F., Murray, H. M., Elbashir, S., Cantley, W., Foster, D., Jayaraman, M., Chappell, A. E., Manoharan, M., Swayze, E. E., and Crooke, S. T. (2013) Lipid Nanoparticles Improve Activity of Single-Stranded siRNA and Gapmer Antisense Oligonucleotides in Animals. *ACS Chem. Biol. 8*, 1402−1406.
(38) Nair, J. K., Willoughby, J. L. S., Chan, A., Charisse, K., Alam, M. R., Wang, Q., Hoekstra, M., Kandasamy, P., Kel'in, A. V., Milstein, S., Taneja, N., O'Shea, J., Shaikh, S., Zhang, L., van der Sluis, R. J., Jung, M. E., Akinc, A., Hutabarat, R., Kuchimanchi, S., Fitzgerald, K., Zimmermann, T., van Berkel, T. J. C., Maier, M. A., Rajeev, K. G., and Manoharan, M. (2014) Multivalent N-Acetylgalactosamine-Conjugated siRNA Localizes in Hepatocytes and Elicits Robust RNAi-Mediated Gene Silencing. *J. Am. Chem. Soc. 136*, 16958−16961.
(39) Shi, Z.-D., Wei, C.-Q., Lee, K., Liu, H., Zhang, M., Araki, T., Roberts, L. R., Worthy, K. M., Fisher, R. J., Neel, B. G., Kelley, J. A., Yang, D., and Burke, T. R. (2004) Macrocyclization in the Design of Non-Phosphorus-Containing Grb2 SH2 Domain-Binding Ligands. *J. Med. Chem. 47*, 2166−2169.
(40) Gao, Y., Luo, J., Yao, Z.-J., Guo, R., Zou, H., Kelley, J., Voigt, J. H., Yang, D., and Burke, T. R. (2000) Inhibition of Grb2 SH2 Domain Binding by Non-Phosphate-Containing Ligands. 2. 4-(2-Malonyl)-phenylalanine as a Potent Phosphotyrosyl Mimetic. *J. Med. Chem. 43*, 911−920.
(41) Rye, C. S., and Baell, J. B. (2005) Phosphate Isosteres in Medicinal Chemistry. *Curr. Med. Chem. 12*, 3127−3141.
(42) Manoharan, M., Rajeev, K., Zlatev, I., Swayze, E. E., Prakash, T. P., Lima, W. (2011) Stabilizing 5′-cap structures for small RNAs for therapeutic use, WO2011133871.
(43) Brown, H. C., McDaniel, D. H., Hafliger, O. Braude, E. A., and Nachod, F. C. (1955) *Determination of Organic Structures by Physical Methods*, Academic Press, New York.
(44) Reddy, M. R., and Erion, M. D. (2001) Calculation of Relative Binding Free Energy Differences for Fructose 1,6-Bisphosphatase Inhibitors Using the Thermodynamic Cycle Perturbation Approach. *J. Am. Chem. Soc. 123*, 6246−6252.
(45) Fiandor, J., García-López, M. T., and De las Heras, F. G. (1989) Synthesis of 5′-C-Chain-Extended Uridines by Reaction of 5′-Halonucleosides with Malonic Acid Type Derivatives. *Nucleosides Nucleotides 8*, 1325−1334.
(46) Kurosu, M., and Li, K. (2009) Synthetic studies towards the identification of novel capuramycin analogs with mycobactericidal activity. *Heterocycles 77*, 217−225.
(47) Kurosu, M., Li, K., and Crick, D. C. (2009) Concise Synthesis of Capuramycin. *Org. Lett. 11*, 2393−2396.
(48) Aleiwi, B. A., and Kurosu, M. (2012) A reliable Pd-mediated hydrogenolytic deprotection of BOM group of uridine ureido nitrogen. *Tetrahedron Lett. 53*, 3758−3762.

DOI: 10.1021/acschembio.5b00654
ACS Chem. Biol. 2016, 11, 953−960

(49) Verheyden, J. P. H., and Moffatt, J. G. (1970) Halo sugar nucleosides. I. Iodination of the primary hydroxyl groups of nucleosides with methyltriphenoxyphosphonium iodide. *J. Org. Chem. 35*, 2319−2326.
(50) Bagshaw, R. D., Pasternak, S. H., Mahuran, D. J., and Callahan, J. W. (2003) Nicastrin is a resident lysosomal membrane protein. *Biochem. Biophys. Res. Commun. 300*, 615−618.
(51) Fujiwara, Y., Furuta, A., Kikuchi, H., Aizawa, S., Hatanaka, Y., Konya, C., Uchida, K., Yoshimura, A., Tamai, Y., Wada, K., and Kabuta, T. (2013) Discovery of a novel type of autophagy targeting RNA. *Autophagy 9*, 403−409.
(52) Heydrick, S. J., Lardeux, B. R., and Mortimore, G. E. (1991) Uptake and degradation of cytoplasmic RNA by hepatic lysosomes. Quantitative relationship to RNA turnover. *J. Biol. Chem. 266*, 8790−8796.
(53) Frank, F., Sonenberg, N., and Nagar, B. (2010) Structural basis for 5′-nucleotide base-specific recognition of guide RNA by human AGO2. *Nature 465*, 818−822.
(54) Pettersen, E. F., Goddard, T. D., Huang, C. C., Couch, G. S., Greenblatt, D. M., Meng, E. C., and Ferrin, T. E. (2004) UCSF Chimera—A visualization system for exploratory research and analysis. *J. Comput. Chem. 25*, 1605−1612.
(55) Elkayam, E., Kuhn, C.-D., Tocilj, A., Haase, A. D., Greene, E. M., Hannon, G. J., and Joshua-Tor, L. (2012) The Structure of Human Argonaute-2 in Complex with miR-20a. *Cell 150*, 100−110.
(56) Chen, C., Ridzon, D. A., Broomer, A. J., Zhou, Z., Lee, D. H., Nguyen, J. T., Barbisin, M., Xu, N. L., Mahuvakar, V. R., Andersen, M. R., Lao, K. Q., Livak, K. J., and Guegler, K. J. (2005) Real-time quantification of microRNAs by stem−loop RT−PCR. *Nucleic Acids Res. 33*, e179.

DOI: 10.1021/acschembio.5b00654
ACS Chem. Biol. 2016, 11, 953−960